Geological Survey of Japan Cruise Report No. 23, p. 1-17, 1994

I. OUTLINE OF THE CRUISE GH83-3 IN THE PENRHYN BASIN, SOUTH PACIFIC

Akira Usui, Masato Nohara, Yoshihisa Okuda, Akira Nishimura, Toshitsugu Yamazaki, Yoshiki Saito, Jun-ichi Miyazaki, Katsuya Tsurusaki, Tetsuo Yamazaki*, Kenichi Harada**, Chi-Won Lee*** and Peter Fleming†*

Introduction

The Geological Survey of Japan (GSJ) has carried out nine research cruises of R/V Hakurei-Maru on marine mineral resources in the Central Pacific Basin since 1974. The Cruise GH83-3 conducted in 1983 is the final phase of the second five-year program "Geological Study of Deep-Sea Mineral Resources" (1979 to 1983) funded by the Agency of Industrial Science and Technology. The objective of this research program is to clarify geological background which affects the regional and local variations of various characteristics of manganese nodule deposits along the Wake-Tahiti Transect (from the Mid-Pacific Mountains, the Central Pacific Basin, the Manihiki Plateau, to the Penrhyn Basin, South Pacific; Fig. I-1). Seven GSJ scientists, five visiting scientists from Yamagata University, the National Institute for Resources and Environments, Japan (formerly National Research Institute for Pollution and Resources), Korea Institute of Geology, Mining and Materials (formerly Korea Institute of Energy and Resources), and Technical University of Clausthal-Zellerfeld, Germany, and eight students from five Japanese universities participated in the cruise (Table I-1). The results of the previous cruises, GH80-1 (Mizuno and Nakao, 1982), GH80-5 (Nakao and Moritani, 1984), GH81-4 (Nakao, 1986), and GH82-4 (Usui, 1992) have been published as GSJ Cruise Reports (see in references) and in other scientific journals (Usui, 1983; Yamazaki, 1986; Usui *et al.*, 1987; Nishimura, 1990; Yamazaki *et al.*, 1991, Usui *et al.*, 1993 and others).

Schedule and Area of Study

The geological research vessel *Hakurei-Maru* commanded by Captain H. Okumura set sail from Funabashi Port, Tokyo Bay on August 8, 1983 for the survey area in the Penrhyn Basin, South Pacific. She called at Papeete, Tahiti on September 6 between two legs and returned to Funabashi on October 6 of the same year. The results of survey for sixty days of the cruise is shown in Table I-2.

* National Institute for Resources and Environment, Tsukuba
** Yamagata University, Yamagata
*** Korea Institute of Geology, Mining and Materials, Korea
† Technical University of Clausthal-Zellerfeld, Germany

Keywords: Geological Survey of Japan, manganese nodule, geophysics, geochemistry, deep-sea sediments, seismic profile, South Pacific, Manihiki Plateau, Hakurei-Maru, Penrhyn Basin

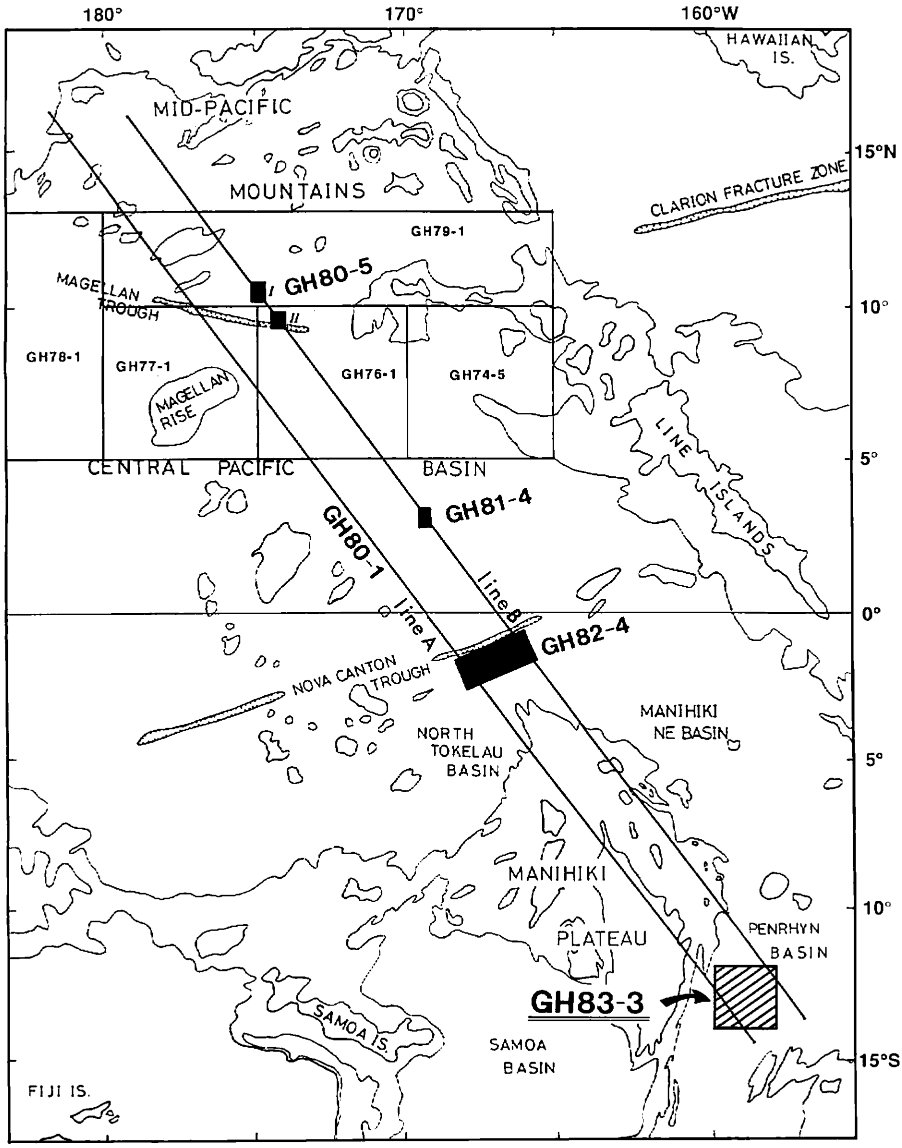

Fig. 1-1 Survey areas of GH83-3 Cruise (marked with an arrow) and previous survey areas of the first and second 5-year GSJ programs. Contours 2000 and 2600 fathoms in water depth (modified from Chase *et al.*, 1977a and 1977b).

Table I-1 List of onboard scientific staff of the Cruise GH83-3.

Name	Organization	Position and speciality *
Masato Nohara	Geological Survey of Japan	chief scientist: geochemistry
Yoshihisa Okuda	Geological Survey of Japan	co-chief scientist: sedimentology
Akira Nishimura	Geological Survey of Japan	scientist; sedimentology
Akira Usui	Geological Survey of Japan	scientist; geochemistry and mineralogy
Toshitsugu Yamazaki	Geological Survey of Japan	scientist; geology and geophysics
Yoshiki Saito	Geological Survey of Japan	scientist; sedimentology
Junichi Miyazaki	Geological Survey of Japan	scientist; topography
Kenichi Harada	Yamagata University	visiting scientist; geology
Lee Chi Won	Korea Institute of Geology, Mining, and Materials	visiting scientist; geology
Peter Fleming	Clausthal Technical University, Germany	visiting scientist; geochemistry
Eiichirou Nishiyama	Chiba University	student; technical assistant
Yoshiyuki Murata	Kobe University	student; technical assistant
Kazushi Kuroki	Ryukyu University	student; technical assistant
Hisayoshi Kasahara	Ryukyu University	student; technical assistant
Takanori Hara	Ryukyu University	student; technical assistant
Hiroyuki Ogura	Ryukyu University	student; technical assistant
Shigeyoshi Iiboshi	Kumamono University	student; technical assistant
Ryoji Yoshidome	Kyoto University	student; technical assistant

* in 1983

The study area is located in the southwestern part of the Penrhyn Basin in the South Pacific to the east of the Manihiki Plateau, which was selected based on previous manganese nodule data on the Wake-Tahiti Transect of the GH80-1 cruise (Mizuno and Nakao, 1982) and earlier investigations by other institutions (Monzier and Missegue, 1977; Glasby, 1981). The first leg was spent for a reconnaissance survey in a box (12-14°S, 158-160°W) and the second leg for a small-scale sampling within a detailed survey area (12°50′S-13°30′S, 158°50′W-159°30′W). Figure I-2 is the topographic map of the GH83-3 area compiled by J. Miyazaki (GSJ). Sample locations are plotted on the topographic maps of the whole area (Fig. I-2) and of the detailed survey area (Fig. I-3).

Methods

The general survey methods are similar to those in the previous Hakurei-Maru cruises (Table I-3). More details of study are described in the following chapters in this volume. In the first leg, bottom sampling was done every 30-mile grids by a set of two free-fall grabs and one wire-lined sampler (a piston corer installed with a heat-flow meter or a box corer with one-shot camera), along parallel lines to the Trough axis at 10-mile intervals (Fig. I-4). The second leg includes small-scale (around 1-km intervals) sampling, sea-bed photography and dredge in the detailed survey area. A table of preliminary results of on-site observation and description of manganese nodule deposits is shown in Appendix I-1.

Table I-2 Records of survey and observation of Cruise GH83-3.

Date		Weather	Crusing time	Cruising mileage	Works
Aug.	8	fine/cloudy	10.0 hr	108.3 n.m.	leave Funabashi port (2:00 pm)
	9	fine/cloudy	24.0	357.7	geophysical survey in transit*
	10	fine/cloudy	24.0	340.0	geophysical survey in transit*
	11	fine/cloudy	23.5	338.6	geophysical survey in transit*
	12	fine/cloudy	23.5	337.6	geophysical survey in transit*
	13	fine/cloudy	23.5	324.5	geophysical survey in transit*
	14	fine/cloudy	23.5	316.4	geophysical survey in transit*
	15	cloudy	23.5	310.6	geophysical survey in transit*
	16	fine/cloudy	23.5	318.5	geophysical survey in transit*
	17	fine	23.5	332.0	geophysical survey in transit*
	17	cloudy	23.5	323.6	geophysical survey in transit*
	18	fine/cloudy	23.5	311.8	geophysical survey in transit*
	19	fine/cloudy	24.0	309.1	geophysical survey in transit*
	20	fine/cloudy	24.0	324.1	geophysical survey in transit*
	21	fine/cloudy	24.0	266.2	geophysical survey ** and sampling (St.3901)
	22	cloudy	24.0	161.9	geophysical survey ** and sampling (Sts.3902-3903)
	23	fine/cloudy	24.0	170.3	geophysical survey ** and sampling (Sts.3904-3905)
	24	fine/cloudy	24.0	183.0	geophysical survey ** and sampling (Sts.3906-3907)
	25	fine/cloudy	24.0	164.8	geophysical survey ** and sampling (Sts.3908-3909)
	26	fine/cloudy	24.0	158.2	geophysical survey ** and sampling (Sts.3910-3911)
	27	fine/cloudy	24.0	170.4	geophysical survey ** and sampling (St.3903A)
	28	fine/cloudy	24.0	160.4	geophysical survey ** and sampling (Sts.3912-3920)
	29	fine/cloudy	24.0	176.7	geophysical survey ** and sampling (Sts.3921-3922)
	30	fine/cloudy	24.0	163.4	geophysical survey ** and sampling (Sts.3923-3924)
	31	fine/cloudy	24.0	155.3	geophysical survey ** and sampling (Sts.3925-3930)
Sept.	1	fine/cloudy	24.0	185.8	geophysical survey ** and sampling (Sts.3931-3936)
	2	fine/cloudy	24.0	232.4	geophysical survey ** and sampling (Sts.3937-3944)
	3	fine/cloudy	24.0	226.4	geophysical survey ** and sampling (Sts.3945-3951)
	4	fine/cloudy	24.0	256.5	geophysical survey ** and sampling (St.3952)
	5	fine/cloudy	24.0	326.1	geophysical survey *
	6	fine	9.5	77.4	arrive at Papeete (9:00 am)
	7	fine/cloudy		0.0	in port
	8	fine/cloudy		0.0	in port
	9	fine/cloudy		0.0	in port
	10	fine/cloudy		0.0	in port
	11	fine/cloudy		0.0	in port
	12	fine/cloudy	8.0	106.3	leave Papeete (2:00 pm) & geophysical survey*
	13	fine/cloudy	24.0	351.6	geophysical survey**
	14	rainy	24.0	249.2	geophysical survey ** and sampling (Sts.3953-3960)
	15	rainy	24.0	146.7	geophysical survey ** and sampling (Sts.3961-3975)
	16	fine/cloudy	24.0	158.7	geophysical survey ** and sampling (Sts.3976-3990)
	17	fine/cloudy	24.0	165.3	geophysical survey ** and sampling (St.3921A)
	18	fine/cloudy	24.0	135.9	geophysical survey ** and sampling (Sts.3991-4005)
	19	fine/cloudy	24.0	116.9	geophysical survey ** and sampling (Sts.4006-4020)
	20	fine/cloudy	24.0	127.9	geophysical survey ** and sampling (Sts.4021-4028)
	21	fine/cloudy	24.0	194.9	geophysical survey ** and sampling (Sts.4029-4031)
	22	fine/cloudy	24.5	366.5	geophysical survey in transit*
	23	fine/cloudy	24.5	371.2	geophysical survey in transit*
	24	fine/cloudy	24.5	380.5	geophysical survey in transit*
	25	fine/cloudy	24.5	384.4	geophysical survey in transit*
	26	cloudy	24.5	363.4	geophysical survey in transit*
	28	rainy	24.5	370.8	geophysical survey in transit*
	29	fine/cloudy	24.5	376.0	geophysical survey in transit*
	30	cloudy	24.5	361.4	geophysical survey in transit*
Oct.	1	fine/cloudy	24.5	351.4	geophysical survey in transit*
	2	fine/cloudy	24.5	362.3	geophysical survey in transit*
	3	fine/cloudy	24.0	359.0	geophysical survey in transit*
	4	cloudy	24.0	351.1	geophysical survey in transit*
	5	fine/cloudy	17.5	219.2	geophysical survey in transit*
	6	cloudy	1.5	6.5	arrive at Funabashi Port (9:00 am)

Note: * = magnetic measurement and gravity measurement.
** = continuous reflection profiling, magnetic and gravity measurements.
Sampling includes sea-bed photography and heat flow measurement.

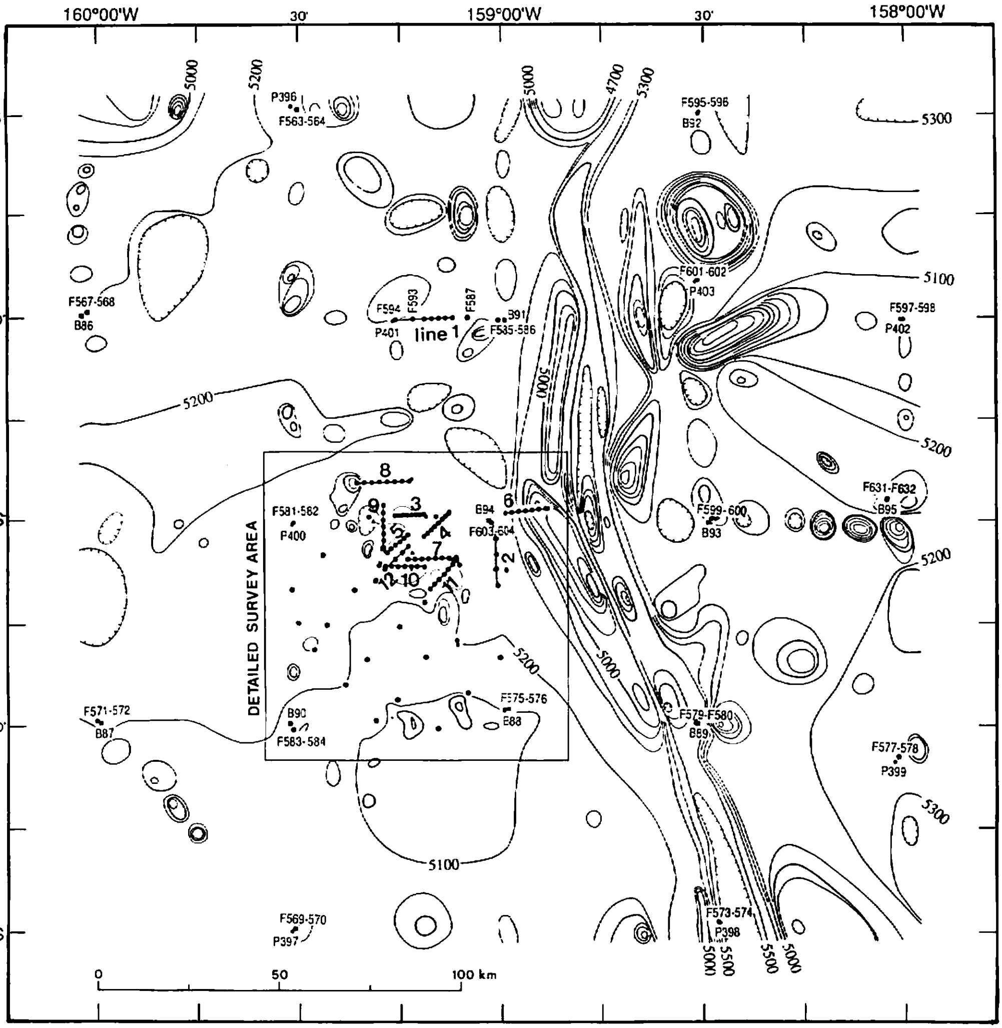

Fig. 1-2 Sampling stations and topography of the GH83-3 area. The base topographic map was compiled by Jun-ichi Miyazaki, GSJ.

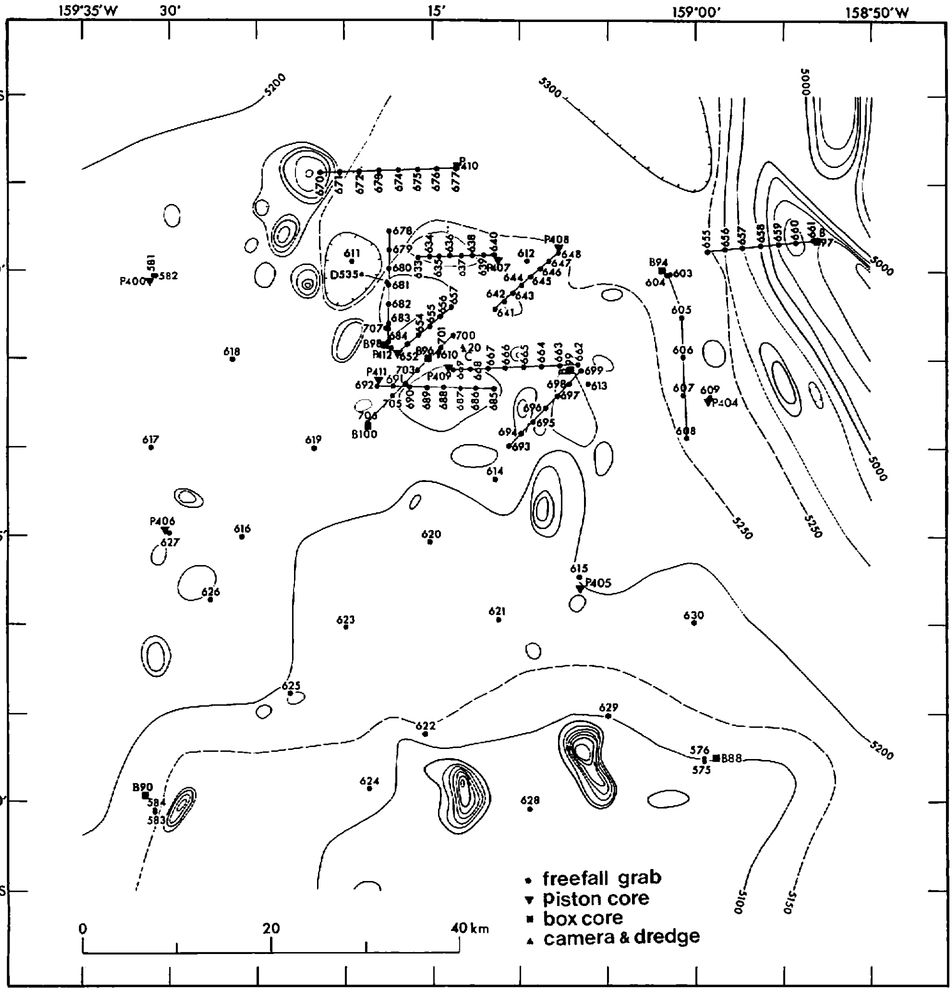

Fig. I-3 Sample locations in the detailed survey area.

Table I-3 Survey methods and results of Cruise GH83-3.

Positioning by NNSS	13878.0 n.m.
Bathymetric survey by 12kHz PDR	13878.0 n.m.
Subbottom profiling by 3.5kHz SBP	13878.0 n.m.
Gravimetric survey by on-board gravimeter	13878.0 n.m.
Continuous seismic reflection profiling by air-gun	2526.4 n.m.
Magnetic survey by proton magnetometer	7117.8 n.m.
Seismic refraction survey by sono-buoy	57.3 n.m.
Nodule sampling by free-fall grab with camera	146 stations (FG563-708)
Nodule sampling by dredge	1 station (D535)
Sediment sampling by box corer	16 stations (B85-100)
Sediment sampling by piston corer	17 stations (P396-412)
Heat flow measurement	17 stations (H90-H106)
Deep-sea photography	1 station (C20)
Geotechnical mesurements	2 stations (EM1-EM2)

Note: Right column shows total mileage of survey and number of stations.

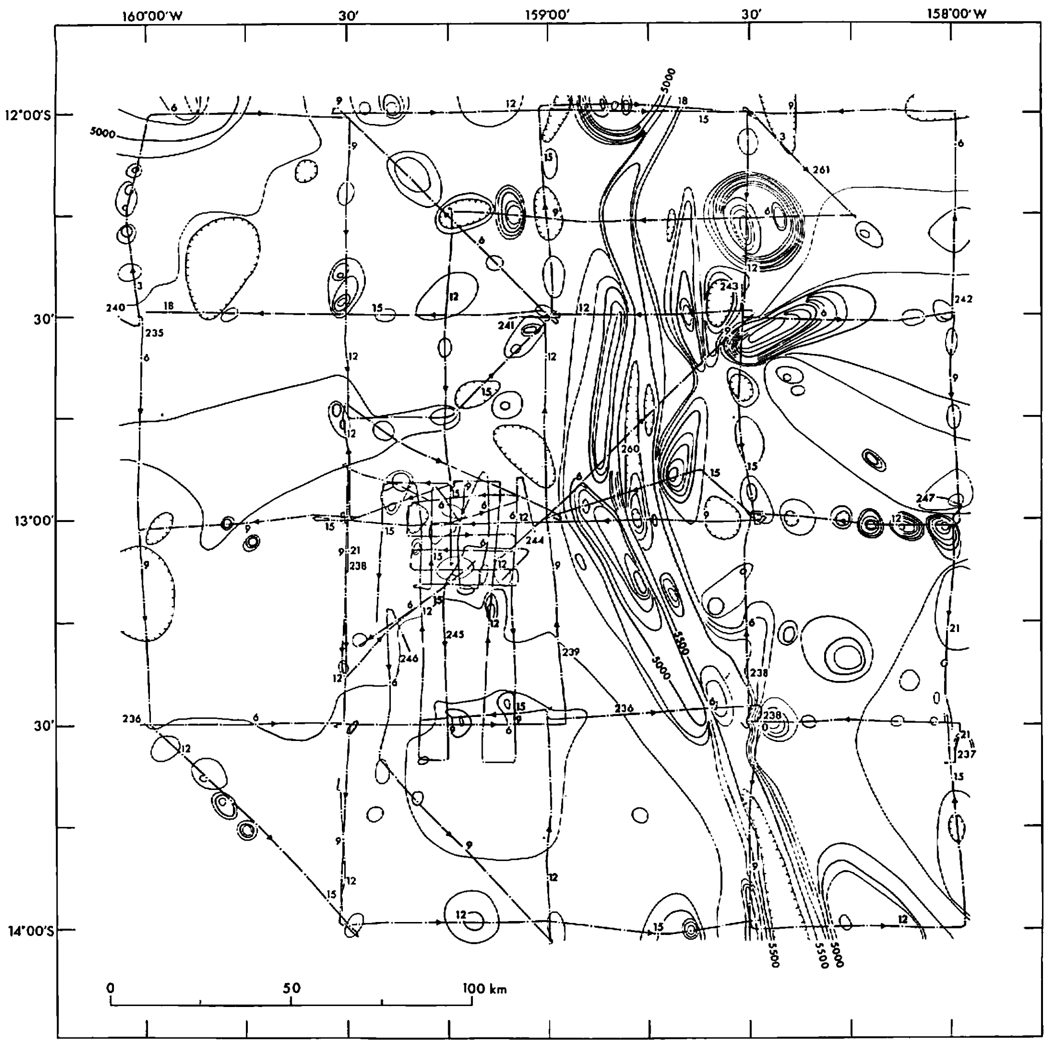

Fig. I-4 Ship tracks of seismic survey by 3.5 kHz SBP and air guns.

Summary of results

Bathymetric survey with a single-beam echo sounder revealed general topography of the GH83-3 area in the western part of the Penrhyn Basin, where only a large-scale topographic map (Chase *et al.*, 1977a and 1977b) had been available. An NNW-SSE trending trough and ridge system and rolled basin floors characterize conspicuous figures of sea floor topography of the area (Okuda *et al.*, Chapter II). The eastern basin to the trough is characterized by rugged sea floor associated with many hills and depressions, whereas the western basin shows relatively flat sea floors at depths between 5100 and 5300 m. The northward slight increase of free-air gravity anomaly suggests dynamical support of the lithosphere in the northern part of the area

(Yamazaki and Okuda, Chapter XIII).

The small amplitude and short wave length of magnetic anomalies support the earlier idea that the Penrhyn Basin belongs to the Cretaceous Magnetic Quiet Zone (Yamazaki and Okuda, Chapter XIII). The trough and ridge system at the center of the area may be most probably a paleo-rift formed during the Cretaceous sea floor spreading (Chapters II and XIII).

Okuda and Miyazaki (Chapter II) and Nishimura *et al.* (Chapter III) present general geologic structure and sedimentary history of the Penrhyn Basin based on air-gun seismic and 3.5 kHz subbottom profiles (SBP). Laminated semi-opaque acoustic layers dominate in the western basin, which are often deformed by later tectonic movements (Chapter II). The layers are sub-divided according to SBP patterns into Units I, II and III (Nishimura *et al.*, Chapter III) which are in agreement with lithologic units I, II and III described from recovered piston cores (Nishimura and Saito, Chapter IV).

Lithology (Chapters IV and V), microfossils (Chapter IV), paleomagnetism (Chapter VI), and chemical composition (Chapter VII) of deep-sea sediments from box cores, piston cores and free-fall grabs were studied in relation to sedimentary history. Nishimura and Saito (Chapter IV) found a wide-spread Paleogene long-term sedimentary hiatus between the Unit I and Units II in most of piston cores from the area, which may have promoted abundant nodule deposits. Yamazaki (Chapter VI) estimates the paleolatitude from magnetic inclination of the cores in agreement with reported plate motions since the Cretaceous time.

Shipboard description of manganese nodules on sea beds and buried within core sediments reveal a regional and small-scale variation pattern of manganese nodule facies in relation to topography and subbottom sediments (Usui, Chapter VIII). Abundant hydrogenetic manganese nodules and rarely crusts have formed since the Paleogene or Cretaceous, being promoted by strengthened flow of the Antarctic Bottom Water into the basin. Facies of manganese deposits are classified into Facies A (small irregular nodules), B (large spherical nodules) and C (crusts on claystones). The regional distribution pattern of these facies in the detailed area is consistent with that of surface sediment Units I, II, and III defined by Nishimura and Saito (Chapter IV). The distribution patterns suggest that the Facies A have formed during deposition of Unit I while Facies B and C have formed before or since the sedimentary hiatus between Units I and II.

Usui and Mita (Chapter IX) describes chemistry, mineralogy and internal growth history of sea-bed and buried nodules. Mineralogical component is vernadite which indicates hydrogenetic origin possibly with a trace amount of diagenetic buserite inside nodules. Bulk chemical characteristics show moderately high Co and Pb contents but low Cu, Ni, and Zn. Internal old nodules within large nodules of Facies B are correlated to the small nodules buried deep in Unit II sediments (Cretaceous to Oligocene, Nishimura and Saito). Nucleus of nodules, for instance, stiff claystones, altered volcanic rocks and hydrothermal manganese oxide, have been lifted up during growth of manganese nodules.

Harada *et al.* (Chapter X) show textural and chemical variation inside nodules on a millimeter scale. Several typical microtextural units of nodule interior are nicely correlated between 8 nodules in the study area. The depth profiles of chemical variation from nodule surface are as well correlated, and the pattern is symmetrical in the top and bottom halves of nodules on sea bed. A monoclinal decrease of Co contents from nodule surface to the interior may be due to decrease of growth rate, if assumed constant Co flux to nodules during growth. They point out the possibility that microstructure and chemistry record changes in marine sedimentary conditions.

Yamazaki (Chapter XI) compares 11 heat flow measurements in the area with those predicted from a recent plate cooling model. The results suggest the age of basement of the Penrhyn Basin area is the late Cretaceous or the middle Cretaceous if reheated by later hot spot activity.

Bottom water temperature at 16 sites indicates the modern southeastward drift of bottom waters at depths below 4800 m, which flows clockwise around the Manihiki Plateau (Yamazaki, Chapter XII). This suggests modern dominant influx of AABW through the Samoan Passage rather than Aitutaki Passage.

Tsurusaki *et al.* (Chapter XIV) measured geotechnical properties of sediments from 7 box cores and 16 piston cores, and describe downcore variations of shear strength and water contents. Water content decreases but shear strength increases with depth from the sediment surface, and they are inversely correlated. The downcore changes are greatest in the top 20 to 30 cm, but gradually change at deeper sediments. Size distribution of manganese nodules show 4.2 cm median diameter.

Acknowledgements

This study was funded by Special Program of the Agency of Industrial Science and Technology, MITI, Japan. We acknowledge the captain and crew of the research vessel *Hakurei-Maru* for their technical assistance and support during the cruise. Drs. A. Mizuno, Ehime University, S. Nakao, M. Tanahashi, K. Iizasa (GSJ) and T. Moritani (Sumitomo Construction Co. Ltd) are appreciated for fruitful discussion and suggestion. The editor expresses special thanks to Dr. J. Eade of the South Pacific Applied Geoscience Commission (SOPAC) Technical Secretariat, Fiji and Dr. T. Sakasegawa of the Metal Mining Agency of Japan, who kindly provided us an opportunity of referencing unpublished official reports on marine mineral resources exploration around the Cook Islands sea area. Ms. M. Kumada is greatly appreciated for her editorial tasks.

Published GSJ Cruise Reports of this program

Cruise GH74-5: No. 4 (1975) *Deep Sea Mineral Resources Investigation in the Eastern Central Pacific Basin.* (Eds.) A. Mizuno & J. Chujo. pp. 103.

Cruise GH76-1: No. 8 (1977) *Deep Sea Mineral Resources Investigation in the Central-Eastern Part of Central Pacific Basin.* (Eds.) A. Mizuno & T. Moritani. pp. 217.

Cruise GH77-1: No. 12 (1979) *Deep Sea Mineral Resources Investigation in the Central-Western Part of Central Pacific Basin.* (Ed.) T. Moritani. pp. 256.

Cruise GH78-1: No. 17 (1981) *Deep Sea Mineral Resources Investigation in the*

Western Part of Central Pacific Basin. (Eds.) T. Moritani & S. Nakao. pp. 281.

Cruise GH79-1: No. 15 (1981) *Deep Sea Mineral Resources Investigation in the Northern Part of Central Pacific Basin.* (Ed.) A. Mizuno. pp. 309.

Cruise GH80-1: No. 18 (1982) *Regional data of marine geology, geophysics, and manganese nodules: the Wake-Tahiti Transect in the Central Pacific.* (Eds.) A. Mizuno. & S. Nakao. pp. 399.

Cruise GH80-5: No. 20 (1984) *Marine geology, geophysics, and manganese nodules in the northern vicinity of the Magellan Trough.* (Eds.) S. Nakao & T. Moritani. pp. 272.

Cruise GH81-4: No. 21 (1986) *Marine geology, geophysics, and manganese nodules around deep-sea hills in the Central Basin.* (Ed.) S. Nakao. pp. 257.

Cruise GH82-4: No. 22 (1992) *Marine Geology, Geophysics and Manganese Nodule Deposits in the Southern Part of the Central Pacific Basin.* (Ed.) A.Usui. pp. 276.

Cruise GH83-3: No. 23 (1993) *Marine Geology, Geophysics and Manganese Nodule Deposits in the Penrhyn Basin, South Pacific.* (Ed.) A.Usui. This volume.

References

Chase, T.E., Menard H.W. and Mammerickx, J. (1977a) *Topography of the South Pacific.* Scripps Inst. Oceanography, La Jolla, California. One sheet map.

———, ——— and ——— (1977b) *Topography of the South Pacific.* Scripps Inst. Oceanography, La Jolla, California. One sheet map.

Nishimura, A. (1992) Sedimentation and hiatuses in the central Pacific Basin: their relationship to manganese nodule formation. In: B.H. Keating and B.R. Bolton (eds.), *Geology and Offshore Mineral Resources of the Central Pacific Basin.* p. 179-203.

Usui, A. (1983) Regional variation of manganese nodule facies on the Wake-Tahiti Transect: morphological, chemical and mineralogical study. *Mar. Geol.*, vol. 54, p. 27-51.

———, Nishimura, A. and Mita, N. (1993) Composition and growth history of surficial and buried manganese nodules in the Penrhyn Basin, Southwestern Pacific. *Marine Geology*, vol. 114, p. 133-153.

———, ———, Tanahashi, M. and Terashima, S. (1987) Local variability of manganese nodule facies on small abyssal hills of the Central Pacific Basin. *Mar. Geol.*, vol. 74, p. 237-275.

Yamazaki, T. (1986) Secondary remanent magnetization of pelagic clay in the South Pacific: application of thermal demagnetization. *Geophys. Res. Lett.*, vol. 13, p. 1438-1441.

———, Katsura, I. and Marumo, K. (1991) Origin of stable remanent magnetization of siliceous sediments in the central equatorial Pacific. *Earth Planet. Sci. Letter.*, vol. 105, p. 81-93.

Appendix 1-1 Results of on-site observations of manganese nodules during the Cruise GH83-3.

Sta. no.	Sample no.	Date (Julian)	Time (GMT)	Location (hit bottom) latitude (°S)	longitude (°W)	Depth (m)	Sed.	Unit I thick. (m)	Manganese nodules morphology	abund. (kg/m)	cov. (%)	Topography
3901	B85	234d	02:50	11°08.93'	161°00.49'	3626	cO	-		0.0	-	top of Manihiki Plateau
3902	FG563		17:34	11°59.30'	159°30.06'	5305	pC	0	ISs, ISPs	21.8	80	flat floor
	FG564		17:40	11°59.17'	159°30.26'	5308	pC	20	IDPs, DPs	15.5	70	flat floor
	FG565		17:43	11°59.10'	159°30.36'	5307	zrC	20	IDPs, IDs	13.2	60	flat floor
	FG566		17:46	11°59.02'	159°30.47'	5307	-	10	Vs	5.9	100	flat floor
	P396		19:19	11°58.82'	159°31.06'	5289	zC	4	ISPs	-	-	flat floor
3903	FG567	235d	00:53	12°59.01'	160°01.23'	5237	pC	0	Ss, ISs	24.1	80	top of a small hill
	FG568		00:58	12°29.14'	160°01.38'	5235	-	0	Fs	0.1	100	top of a small hill
	B86		02:39	12°29.66'	160°02.30'	5155	pC	0	Ss, ISs	21.8	-	top of a small hill
3904	FG569		16:26	13°59.31'	159°30.65'	5170	zC	tr	Ss, ISs	29.8	50	flat floor
	FG570		16:30	13°59.40'	159°30.61'	5176	zrC	tr	Ss, ISs	21.3	60	flat floor
	P397		18:06	13°51.77'	159°31.02'	5176	zC	tr	ISPs	-	-	flat floor
3905	FG571	236d	00:13	13°29.33'	159°59.97'	5204	-	tr	IDs, IDPs	1.3	100	flat floor
	FG572		00:16	13°29.19'	159°59.98'	5208	-	tr	Cs	-	100	flat floor
	B87		01:57	13°29.50'	159°59.47'	5206	-	tr		-	-	flat floor
3906	FG573		16:52	13°58.59'	158°27.82'	5704	zC	7		0.0	0	slope of trough
	FG574		16:57	13°58.54'	158°27.75'	5707	zrC	7	Vs	0.1	0	slope of trough
	P398/H92		18:37	13°58.53'	158°27.69'	5727	zrC	7		-	-	bottom of trough
3907	FG575	237d	23:58	13°27.69'	158°59.53'	5073	-	tr	ISs, IDs	19.2	60	flat floor
	FG576		00:01	13°27.53'	158°59.54'	5087	zrC	tr	Ts, ISs	32.3	70	flat floor
	B88		01:39	13°27.48'	158°58.86'	5124	zrC	tr	ISs	-	-	flat floor
3908	FG577		16:48	13°34.47'	158°01.08'	5294	zC	20	IDPs	0.3	2	flat floor
	FG578		16:52	13°34.62'	158°01.11'	5294	zC	20	IDs, IDPs	0.4	3	flat floor
	P399/H93		18:24	13°35.41'	158°01.64'	5304	-	20	Cs	-	-	flat floor
3909	FG579	238d	00:23	13°29.67'	158°30.99'	5568	-	40	Cs	0.0	100	flat floor near seamount
	FG580		00:26	13°29.67'	158°31.11'	5570	zC	40	IDs, IDPs	3.9	30	flat floor near seamount
	B89		02:28	13°29.72'	158°30.90'	5583	-	40		-	-	flat floor near seamount

Appendix 1-1 (continued)

Sta. no.	Sample no.	Date (Julian)	Time (GMT)	Location (hit bottom) latitude (°S)	longitude (°W)	Depth (m)	Sed.	Unit I thick. (m)	Manganese nodules morphology	abund. (kg/m)	cov. (%)	Topography
3910	FG581		16:25	13°00.31'	159°30.73'	5248	-	20	Cs	-	100	flat floor
	FG582		16:28	13°00.28'	159°30.90'	5248	zrC	20	IDs, IDPs	23.4	50	flat floor
	P400/H94		18:03	13°00.62'	159°31.05'	5242	zrC	20	IDs	-	-	flat floor
3911	FG583		23:51	13°30.56'	159°30.81'	5173	-	0	Ts, IDs	15.4	80	flat floor
	FG584		23:54	13°30.44'	159°30.83'	5178	-	0	Ts, IDs	8.3	80	flat floor
	B90	239d	01:41	13°29.60'	159°31.29'	5196	-	0	Cs	-	100	flat floor
3912	FG585	240d	17:06	12°30.41'	159°00.54'	5349	pC	15	Ts, IDs	28.8	80	flat floor near seamount
	FG586		17:10	12°30.40'	159°00.37'	5349	zrC	15	IDs, Ds	16.6	80	flat floor near seamount
	B91		18:56	12°30.46'	158°59.25'	5345	pC	15	Ts, IDs	18.5	70	flat floor near seamount
3913	FG587		20:57	12°30.03'	159°04.89'	5294	zrC	5	IDPs, IDs	10.0	30	flat floor
3914	FG588		21:13	12°30.05'	159°07.07'	5272	zrC	5	IDs, IDPs	4.6	10	flat floor
3915	FG589		21:24	12°30.11'	159°08.15'	5268	pC	tr	IDPs, IDs	6.7	15	flat floor
3916	FG590		21:34	12°30.13'	159°09.19'	5268	zrC	15	IDs, IDPs	17.4	25	flat floor
3917	FG591		21:44	12°30.19'	159°10.23'	5261	zrC	tr	IDs, IDPs	6.8	-	flat floor
3918	FG592		21:54	12°30.22'	159°11.29'	5260	pC	5	IDs, IDPs	0.6	-	flat floor
3919	FG593		22:09	12°30.25'	159°13.01'	5232	zrC	5	IDs, IDPs	0.8	-	flat floor
3920	FG594		22:29	12°30.33'	159°15.69'	5209	zrC	12	IDs, IDPs	0.2	-	flat floor
	P401/H95		23:56	12°30.56'	159°16.00'	5206	zC	12		-	-	flat floor
3921	FG595	241d	16:26	11°59.96'	158°30.59'	5268	pC	20	Ss, ISs	36.4	-	top of hill
	FG596		16:30	12°00.05'	158°30.48'	5268	-	20	Ss, ISs	24.4	-	top of hill
	B92		18:13	12°00.03'	158°30.64'	5248	zrC	20	Ss, ISs	37.9	70	slope of hill
3922	FG597		23:45	12°30.26'	158°00.23'	4941	zC	20	Ss, Ts	30.9	-	flat floor
	FG598		23:48	12°30.36'	158°00.22'	4938	zC	20	Ss, ISs	27.2	-	flat floor
	P402H96	242d	01:05	12°30.25'	158°00.83'	4950	zC	20		-	-	flat floor
3923	FG599		16:45	12°59.65'	158°28.83'	5098	zrC	tr	Ts, IDPs	20.2	-	rugged floor
	FG600		16:48	12°59.74'	158°28.83'	5101	-	tr	Ts, IDs	18.6	80	rugged floor
	B93		18:34	13°00.27'	158°29.17'	5098	zrC	tr	Ss	-	-	rugged floor

Appendix 1-1 (continued)

Sta. no.	Sample no.	Date (Julian)	Time (GMT)	Location (hit bottom) latitude (°S)	longitude (°W)	Depth (m)	Sed.	Unit I thick. (m)	Manganese nodules morphology	abund. (kg/m)	cov. (%)	Topography
3924	FG601		23:37	12°24.57'	158°30.83'	5341	-	35		-	-	flat floor near seamount
	FG602		23:40	12°24.62'	158°30.76'	5346	zrC	35	Ds, DPs	1.1	5	flat floor near seamount
	P403/H97	243d	01:16	12°24.80'	158°31.15'	5330	zC	35		-	-	flat floor near seamount
3925	FG603		17:48	13°00.21'	159°01.43'	5299	zrC	20	IDPs, IDs	0.4	5	flat floor near seamount
	FG604		17:52	13°00.24'	159°01.60'	5299	zC	20	Ds, IDs	2.7	5	flat floor near seamount
	B94		19:37	12°59.99'	159°01.80'	5289	-	20	IDPs	0.5	-	flat floor near seamount
3926	FG605		22:04	13°02.65'	159°00.77'	5291	zC	tr	Ts, IDPs	17.2	40	flat floor
3927	FG606		22:23	13°04.87'	159°00.72'	5297	zC	tr	Ts, IDPs	17.3	40	flat floor
3928	FG607		22:41	13°06.97'	159°00.69'	5284	zC	5	Ts, IDPs	9.4	40	flat floor
3929	FG608		23:03	13°09.43'	159°00.50'	5268	zrC	10	Ds, IDs	5.8	20	flat floor
3930	FG609		23:30	13°07.10'	158°59.18'	5291	zrC	tr	Ts, Fs	13.3	40	flat floor
	P404/H98	244d	00:56	13°07.25'	158°59.31'	5289	-	tr	IDs	-	-	flat floor
3931	FG610		16:31	13°04.62'	159°14.64'	5217	pC	tr	IDs, IDPs	21.4	70	flat floor
3932	FG611		17:16	12°59.45'	159°19.59'	5271	pC	tr	Ss, ISs	32.5	90	bottom of depression
3933	FG612		18:28	12°59.43'	159°09.55'	5240	zrC	20	IDPs	0.3	-	flat floor
3934	FG613		22:07	13°06.37'	159°06.08'	5207	zrC	20	IDs, IDPs	0.1	10	flat floor
3935	FG614		22:50	13°11.79'	159°11.35'	5231	zrC	10	Ts, IDs	11.5	20	flat floor
3936	FG615		23:42	13°17.31'	159°06.57'	5210	-	tr	IDs, Ts	9.7	10	flat floor
	P405/H99	245d	01:07	13°17.96'	159°06.51'	5238	zrC	tr		0.0	-	flat floor
3937	FG616		16:41	13°15.06'	159°25.83'	5232	pC	tr	ISs, IDs	28.9	80	flat floor, slight rugged
3938	FG617		17:23	13°09.99'	159°31.00'	5274	pC	tr	ISs, IDs	11.5	70	flat floor, slight rugged
3939	FG618		18:08	13°05.02'	159°26.37'	5252	zrC	tr	IDs, Ts	16.3	60	flat floor, slight rugged
3940	FG619		18:54	13°10.03'	159°21.73'	5224	pC	tr	ISs, IDs	11.1	70	flat floor, slight rugged
3941	FG620		22:47	13°15.33'	159°15.10'	5173	pC	tr	ISs, IDs	14.8	30	flat floor, slight rugged
3942	FG621		23:26	13°19.75'	159°11.17'	5181	zC	tr	Ts, IDs	12.3	20	flat floor, slight rugged
3943	FG622	246d	00:18	13°26.15'	159°15.44'	5156	pC	tr	ISs, Fs	26.5	80	flat floor near seamount
3944	FG623		01:01	13°20.15'	159°19.93'	5181	zC	tr	Ts, IDs	25.3	50	flat floor

Appendix I-1 (continued)

Sta. no.	Sample no.	Date (Julian)	Time (GMT)	Location (hit bottom) latitude (°S)	longitude (°W)	Depth (m)	Sed.	Unit I thick. (m)	Manganese nodules morphology	abund. (kg/m)	cov. (%)	Topography
3945	FG624		16:42	13°29.23'	159°18.62'	5129	pC	tr	IDPs, ISs	5.2	50	rugged floor
3946	FG625		17:23	13°23.86'	159°23.11'	5170	pC	tr	Ts, IDPs	13.0	70	top of hill
3947	FG626		18:04	13°18.61'	159°27.63'	5220	pC	tr	Ss, Ds	19.4	80	f near seamount
3948	FG627		18:32	13°14.85'	159°29.96'	5263	pC	tr	Ss, ISs	29.6	80	flat floor
	P406/H100		19:56	13°14.66'	159°30.16'	5268	pC	tr	IDs	-	-	flat floor
3949	FG628	247d	00:42	13°30.41'	159°09.40'	5073	zrC	20	Ss, ISs	24.5	70	flat floor
3950	FG629		01:29	13°25.11'	159°04.96'	5118	zrC	15	Ss, ISs	6.7	50	foor of seamount
3951	FG630		02:16	13°19.88'	159°00.10'	5191	zC	15	IDs, IDPs	4.9	5	flat floor
3952	FG631		15:32	12°57.06'	158°02.79'	5376	zC	0	Ts, Fs	4.4	10	rugged floor
	FG632		15:36	12°57.02'	158°02.73'	5381	zC	0	Ts, Fs	16.0	30	rugged floor
	B95		17:20	12°57.01'	158°02.70'	5376	zC	0	IDs, Fs	6.8	10	rugged floor
3953	FG633	257d	22:11	12°59.21'	159°15.84'	5192	pC	tr	Ts, ISs	18.5	80	slightly rugged floor
3954	FG634		22:19	12°59.17'	159°15.17'	5170	pC	tr	ISs, IDs	11.7	80	slightly rugged floor
3955	FG635		22:26	12°59.15'	159°14.62'	5180	pC	tr	Ss, IDs	19.7	80	slightly rugged floor
3956	FG636		22:34	12°59.13'	159°13.99'	5192	pC	tr	Ss, ISs	29.1	80	slightly rugged floor
3957	FG637		22:43	12°59.11'	159°13.28'	5194	pC	tr	Ss, ISs	28.6	80	slightly rugged floor
3958	FG638		22:51	12°59.09'	159°12.68'	5215	pC	tr	ISs, IDs	27.1	-	slightly rugged floor
3959	FG639		23:00	12°59.07'	159°12.01'	5230	pC	tr	Ss, ISs	19.2	-	slightly rugged floor
3960	FG640		23:07	12°59.05'	159°11.42'	5228	zrC	tr	Ss, ISs	20.9	80	slightly rugged floor
	P407/H10:	258d	00:31	12°59.38'	159°11.22'	5248	zrC	tr	ISPs	-	-	flat floor
3961	FG641		17:11	13°02.22'	159°11.38'	5222	pC	0	ISPs, IDs	30.3	85	top of hill
3962	FG642		17:20	13°01.78'	159°10.85'	5217	pC	0	ISPs, IDs	-	50	flat floor
3963	FG643		17:28	13°01.31'	159°10.35'	5211	zrC	0	ISs, IDs	14.2	40	flat floor
3964	FG644		17:36	13°00.84'	159°09.84'	5217	zrC	tr	ISs, IDs	11.3	30	flat floor
3965	FG645		17:44	13°00.38'	159°09.32'	5227	zrC	tr	IDs, IDPs	2.2	10	flat floor
3966	FG646		17:52	12°59.89'	159°08.80'	5232	zrC	15	IDs, IDPs	3.0	-	flat floor
3967	FG647		18:00	12°59.43'	159°08.29'	5242	zrC	20	IDs, ISs	0.6	5	flat floor

Appendix I-1 (continued)

Sta. no.	Sample no.	Date (Julian)	Time (GMT)	Location (hit bottom) latitude (°S)	longitude (°W)	Depth (m)	Sed.	Unit I thick. (m)	Manganese nodules morphology	abund. (kg/m)	cov. (%)	Topography
3968	FG648		18:09	12°58.93'	159°07.76'	5255	zrC	30	IDs, Ds	0.5	5	flat floor
3968	P408/H102		19:35	12°58.65'	159°07.68'	5258	zC	30	IDs, IDPs	-	-	flat floor
3969	FG649		23:18	13°02.09'	159°13.93'	5206	-	15	ISs, Ss	2.5	85	flat top of rolled floor
3970	FG650		23:27	13°02.62'	159°14.54'	5232	-	tr	Cs	0.0	100	flat floor
3971	FG651		23:35	13°03.15'	159°15.15'	5227	-	tr	Ts, IDs	8.1	40	flat floor
3972	FG652		23:43	13°03.65'	159°15.78'	5211	zrC	tr	Ss, ISs	14.7	80	flat floor
3973	FG653		23:51	13°04.15'	159°16.42'	5225	-	tr	Ts, Fs	15.6	70	flat floor
3974	FG654		23:59	13°04.67'	159°16.97'	5211	pC	0	Ss, IDPs	27.6	80	flat floor
3975	B96	259d	01:59	13°04.93'	159°15.24'	5237	zrC	0	IDs, IDPs	-	-	flat floor
3976	FG655		16:45	12°58.89'	158°59.31'	5268	zC	0	Ss, IDs	14.9	30	foot of seamount
3977	FG656		16:57	12°58.75'	158°58.34'	5176	-	0	IDs	3.6	15	slope of seamount
3978	FG657		17:08	12°58.63'	158°57.33'	5114	zC	0	ISs, IDs	5.0	20	slope of seamount
3979	FG658		17:20	12°58.53'	158°56.30'	5032	zrC	0	ISs, ISPs	26.0	80	slope of seamount
3980	FG659		17:31	12°58.44'	158°55.29'	4755	zcC	0	Ss, Ds	50.3	85	slope of seamount
3981	FG660		17:42	12°58.33'	158°54.29'	4648	zcC	0	ISs, ISPs	33.2	90	top of seamount
3982	FG661		17:53	12°58.20'	158°53.30'	4714	-	0	Cs	0.0	100	top of seamount
3982	B97		19:26	12°58.21'	158°53.06'	4714	cC	0	IDs, ISs	26.9	90	top of seamount
3983	FG662		22:59	13°05.30'	159°06.66'	5205	zrC	35	IDs, IDPs	0.2	5	flat floor
3984	FG663		23:08	13°05.35'	159°07.70'	5202	zrC	20	IDs, IDPs	4.4	25	flat floor
3985	FG664		23:17	13°05.39'	159°08.72'	5206	zrC	15	IDs, IDPs	8.8	30	flat floor
3986	FG665		23:26	13°05.45'	159°09.75'	5201	pC	tr	IDs, ISs	31.7	50	flat floor
3987	FG666		23:35	13°05.49'	159°10.79'	5237	zrC	0	IDs, Ds	-	50	depression in flat floor
3988	FG667		23:44	13°05.52'	159°11.77'	5231	zrC	tr	Ts, IDs	17.8	40	depression in flat floor
3989	FG668		23:53	13°05.56'	159°12.79'	5206	pC	tr	Ts, Ss	12.3	70	flat floor, gently rolled
3990	FG669	260d	00:02	13°05.60'	159°13.79'	5201	zrC	tr	Ss, ISs	26.6	85	flat floor, gently rolled
	P409/H103		01:23	13°05.56'	159°14.06'	5186	zrC	tr		0.0	-	flat floor, gently rolled
3991	FG670	261d	16:45	12°54.40'	159°21.42'	4842	-	0	Cs	0.0	100	top of hill

Appendix I-1 (continued)

Sta. no.	Sample no.	Date (Julian)	Time (GMT)	Location (hit bottom) latitude (°S)	longitude (°W)	Depth (m)	Sed.	Unit I thick. (m)	Manganese nodules morphology	abund. (kg/m)	cov. (%)	Topography
3992	FG671		16:57	12°54.34'	159°20.28'	5237	pC	tr	Fs, ISs	18.7	80	foot of hill
3993	FG672		17:08	12°54.32'	159°19.17'	5266	zrC	20	Ss, IDs	3.0	30	flat floor
3994	FG673		17:19	12°54.27'	159°18.05'	5276	pC	tr	Ts, IDs	17.5	40	flat floor
3995	FG674		17:30	12°54.23'	159°16.93'	5299	-	0	Cs	0.0	100	flat floor
3996	FG675		17:41	12°54.20'	159°15.84'	5253	pC	tr	Ss, ISs	29.8	70	flat floor
3997	FG676		17:52	12°54.16'	159°14.76'	5279	pC	tr	IDs, IDPs	10.5	50	flat floor
3998	FG677		18:04	12°54.15'	159°13.66'	5268	pC	tr	IDs, IDPs	5.7	70	flat floor
	P410/H104		19:29	12°54.00'	159°13.49'	5278	zrC	tr	IDPs	-	-	flat floor
3999	FG678		23:30	12°57.72'	159°17.49'	5299	pC	20	ISs, Ss	35.2	90	flat floor
4000	FG679		23:40	12°58.80'	159°17.47'	5248	pC	tr	ISs, Ss	39.5	-	rugged floor
4001	FG680		23:50	12°59.87'	159°17.49'	5268	pC	tr	ISs, IDPs	36.7	-	foot of hill
4002	FG681		23:59	13°00.85'	159°17.50'	5214	-	tr	Ss, Ds	3.0	80	top of hill
4003	FG682	262d	00:09	13°01.95'	159°17.50'	5176	pC	tr	Ss, IDs	22.9	80	slope of hill
4004	FG683		00:19	13°02.99'	159°17.50'	5135	zrC	tr	Ts, IDs	8.9	40	slope of hill
4005	FG684		00:29	13°04.03'	159°17.51'	5217	zrC	tr	ISs, IDs	16.2	80	flat floor
	B98		02:11	13°04.16'	159°17.69'	5227	-	tr		-	-	flat floor
4006	FG685		16:44	13°02.22'	159°11.43'	5212	-	tr	Ts, IDs	-	70	rolled floor
4007	FG686		16:55	13°06.60'	159°12.48'	5173	zrC	tr	Ss, IDs	28.4	50	rolled floor
4008	FG687		17:03	13°06.63'	159°13.37'	5185	-	tr	Ss, IDs	-	60	rolled floor
4009	FG688		17:12	13°06.56'	159°14.34'	5185	-	tr	Ts, IDs	24.5	70	rolled floor
4010	FG689		17:21	13°06.58'	159°15.29'	5207	zC	tr	Ts, IDs	20.0	50	rolled floor
4011	FG690		17:31	13°06.53'	159°16.27'	5181	pC	tr	Ts, IDs	25.3	60	rolled floor
4012	FG691		17:40	13°06.49'	159°17.23'	5209	pC	tr	Ts, IDs	26.6	70	rolled floor
4013	FG692		17:48	13°06.48'	159°18.13'	5204	pC	tr	ISs, IDPs	8.0	20	rolled floor
	P411/H105		19:13	13°06.16'	159°17.01'	5217	zrC	tr	IDs, IDPs	-	-	rolled floor
4014	FG693		23:14	13°09.90'	159°10.57'	5222	pC	10	IDs, ISs	4.3	20	flat floor
4015	FG694		23:26	13°09.18'	159°09.88'	5141	-	0	Cs	1.0	100	top of hill

Appendix I-1 (continued)

Sta. no.	Sample no.	Date (Julian)	Time (GMT)	Location (hit bottom) latitude (°S)	longitude (°W)	Depth (m)	Sed.	Unit I thick. (m)	Manganese nodules morphology	abund. (kg/m)	cov. (%)	Topography
4016	FG695		23:36	13°08.50'	159°09.21'	5042	-	0	Cs	0.1	100	top of hill
4017	FG696		23:47	13°07.75'	159°08.49'	5211	-	0	Cs	0.0	100	flat floor
4018	FG697		23:57	13°07.05'	159°07.82'	5191	zrC	10		0.0	100	flat floor
4019	FG698	263d	00:07	13°06.36'	159°07.15'	5194	zrC	15	IDs, IDPs	2.8	15	flat floor
4020	FG699		00:18	13°05.64'	159°06.47'	5206	zrC	15	IDs, IDPs	1.4	10	flat floor
	B99		01:56	13°05.52'	159°07.06'	5204	zC	15	IDs, IDPs	-	-	flat floor
4021	FG700		17:25	13°03.67'	159°13.82'	5230	-	0	IDs, Fs	1.0	100	flat floor
4022	FG701		17:37	13°04.34'	159°14.54'	5226	pC	0	IDs	1.4	50	flat floor
4023	FG702		17:46	13°05.01'	159°15.18'	5230	-	0	Cs, Fs	0.1	100	flat floor
4024	FG703		17:54	13°05.63'	159°15.82'	5199	zrC	0	Ss, ISs	9.0	70	slope of hill
4025	FG704		18:04	13°06.35'	159°16.53'	5211	pC	0	Ts, IDs	12.2	70	flat floor, gently rolled
4026	FG705		18:14	13°07.05'	159°17.26'	5209	pC	tr	Ts, IDs	20.1	-	flat floor, gently rolled
4027	FG706		18:31	13°08.60'	159°18.67'	5224	zrC	tr	Ts, IDs	19.0	-	flat floor
	B100		20:09	13°08.80'	159°18.67'	5220	pC	tr	Ts, Ss	19.0	40	flat floor
4028	C20	264d	02:08	13°04.50'	159°13.12'	5235	-	0	IDs, IDPs	-	-	flat floor
4029	FG707		15:38	13°03.27'	159°17.65'	5167	zrC	0	ISs, IDs	22.2	80	slope of hill
	FG708		15:43	13°03.30'	159°17.51'	5160	pC	0	IDs, IDPs	16.5	70	slope of hill
4030	P412/H106		17:10	13°04.40'	159°17.31'	5217	zrC	0	ISs, IDPs	-	-	flat floor
4031	D535		21:27	13°00.64'	159°17.59'	5222	-	0	Ss, Ds	-	-	top of hill

Notes:

Sample no.: FG=free-fall grab, B=box core, P=piston core, D=dredge, C=towed camera. X means ocurrence of buried nodules.
Unit I: uppermost transparent layer by SBP. thick.=estimated thickness of Unit I, tr=traceable.
Sediment: c=calcareous, z=zeolitic, zr=zeolite-rich, p=pelagic, C=clay, O=ooze
Nodules: abund.=abundance, tr=less than 0.1 kg/m , cov.=sea-floor coverage, R/C/N=rock/crust/nodule.